EAN 2017
55th conference on experimental stress analysis

Optimization of Hexacopter Stability Control with Disturbances in its Stochastic State Space Dynamics Model

I. N. Ibrahim, M. A. Al Akkad and E. V. Sosnovich
Department of Mechatronics and Robotics
Kalashnikov Izhevsk State Technical University
Izhevsk, Russia

ibrncfe@gmail.com, aimanakkad@yandex.ru, ellasosnovich@gmail.com

Keywords: Linear Quadratic Regulator, Stochastic State Space, Hexacopter Dynamics, Disturbances, Nonlinear Control, Coupled and Underactuated Models.

Abstract. In this paper, the behavior of a hexacopter with the existence of disturbances inserted into the equations of motion was explored. These disturbances emulate the motion of a robotic arm attached to the body of the aircraft model. Initially, kinematics and dynamics are described. Then, equations of motion are derived for modeling and disturbances analysis. The derived dynamic model reflects the real motion of the hexacopter with respect to the earth, which is also characterized by nonlinearity, time variance, underactuation and coupling among the equations' variables. The state space method was used to write the equations in addition to decoupling and linearization techniques in order to design the controllers. Finally, PID and LQR controllers and simulation results are presented. Both PID and LQR controllers have been investigated to control the aircraft model. The results of comparison between them indicate that the LQR controller is kind of an optimization technique and used to stabilize the attitude of the hexacopter. It consumes low energy with respect to the PID controller in addition to rejecting the perturbation and noise in the stochastic state space of the aircraft model.

1. Introduction

Nowadays, Drones invade several application domains [1,2,3,20,24,26]. The control of an aerial robot such as a hexacopter requires studying its dynamics in order to account for gravity effects, aerodynamic forces [1,2,21,22,23] and disturbances. This work will focus on the modeling, simulation, and control of a hexacopter type UAV. The reason for choosing a hexacopter is challenging in the control field because it's a highly nonlinear, multivariable, coupled and underactuated system, in addition to its advantages such as high maneuverability and stationary flight [4,5]. Underactuated systems, defined as a mechanical system in which the dimension of the configuration space exceeds that of the control input space, that is, with fewer control inputs than degrees of freedom [2]. Modeling of such a system is not a trivial problem due to the coupled dynamics of the aerial vehicle [3]. The contributions of this work are deriving an accurate and detailed mathematical model of a hexacopter UAV in regard to the earth frame. The equation of motion of the whole system was designed using the Newton-Euler formulation for translational and rotational dynamics of a rigid body [4,5,6,7,8,25,26]. The disturbances are presented as an outdoor environment for simulation and it was considered as a so complicated problem in addition to the stochastic idea in the state space model [9, 10], which is omitted in most of the literature. This paper includes the disturbances, which represent the robotic arm movement of a robotic arm attached to the hexacopter in the

equations of force and moment. Lucia [3] and Hasan [4] work in comparison to this research relied on a complex mechanism through the mathematical modeling of certain arms of fixed design, and adding it to the flying object equations. This is considered limited, complex, and does not cover the changes that may occur in the air, and weather conditions to which the aircraft is exposed in the air far from laboratory conditions. The disturbances have been measured using LabVIEW software and used to build a stochastic state space model [11], which is a simple type of representation with the existence of noise. Two types of control methods were investigated, using proportional integral deferential PID controller and linear quadratic regulator LQR controller in order to get a good response in addition to low energy consumption. Bouabdallah implemented such a type of controller in the closed loop system to stabilize the angular attitude of a UAV [12] [13] [14]. Castillo implemented an LQR controller too, to stabilize a quadcopter in hover situation [15]. Hoffmann et al. used the LQR as a solution to the energy problem in order to apply lower costs on attitude deviations by varying the Q matrix, but this degraded the tracking performance. A good compromise is found in [16]. This paper is structured as follows: initially, kinematics and dynamics are described. Then, equations of motion are derived for modeling and disturbances analysis. Finally, PID and LQR controllers and simulation results are presented. The future work will focus on developing attitude, position, and altitude robust controllers to obtain proper strategies for autopilot stabilization and trajectory control.

2. Reference Systems for the UAV Hexacopter

To describe the hexacopter motion only two reference systems are necessary: earth inertial frame (E-frame) and body-fixed frame (B-frame). The inertial frame is the system that uses the North, East, and Down (NED) coordinates and the origin of this reference system is fixed in one point located on the earth surface as shown in Fig. 1, and the (X, Y, Z) axes are directed to the North, East, and Down, respectively. The mobile frame (X_B, Y_B, Z_B) is the body fixed frame that is centered in the hexacopter center of gravity (CG) and oriented as shown in Fig. 1. The angular position of the body frame with respect to the inertial one is usually defined by means of the Euler angles: roll ϕ, pitch θ, and yaw ψ, where vector: $\sigma = [\phi\ \theta\ \psi]^T$,$\phi\ and\ \theta \in]-\frac{\pi}{2},\frac{\pi}{2}[$; $\psi \in]-\pi,\pi[$. The inertial frame position of the vehicle is given by vector $\xi = [x\ y\ z]^T$ [4, 16, 17]. The transformation from the body frame to the inertial frame is realized by using the well-known rotation matrix C_b^n [16, 17]. while the transformation matrix for angular velocities from the body frame to the inertial one is S [3, 18]. Where $\dot{\sigma} = S\ .\ \Omega$, $\dot{\xi} = C_b^n\ .\ V$, the angular velocity is defined by vector $\Omega = [p\ q\ r]^T$, and the linear velocity is defined by vector $V = [u\ v\ w]^T$ in the body frame.

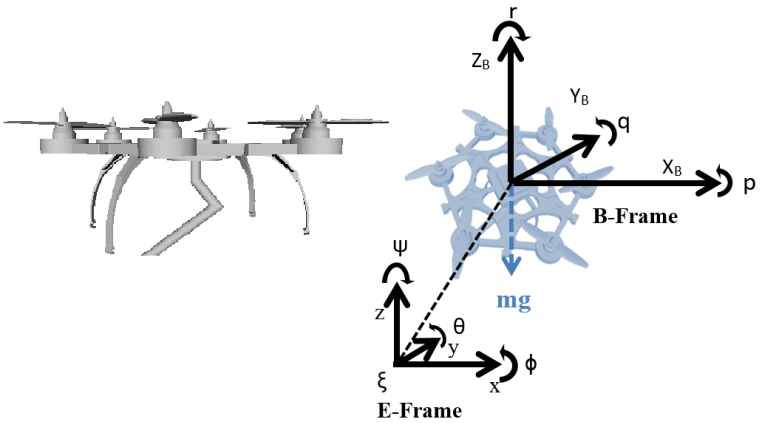

Figure 1. Hexacopter UAV structure and frames.

3. Dynamical Model of Hexacopter

To describe the hexacopter dynamics, that is assumed to be a rigid body and has a symmetrical structure, Newton-Euler equations [3, 18] that govern linear and angular motion are used. This model has the The thrust and torque as in [15] are: $|T_i| = \rho C_T A R^2 \omega_i^2$, and $|Q_i| = \rho C_Q A R^3 \omega_i^2$, Where blade rotation is with angular velocity ω, the blade radius is R, C_T and C_Q are respectively thrust and torque coefficients, ρ is the air density and A is the disc area, while the opposing force to the travelling of the hexacopter in air is the drag force and can be expressed by the following equation at the earth's frame: $F_{AI} = K_{TI}.\dot{\xi}$, where K_{TI} is a diagonal matrix related to the aerodynamic friction constant k_t [15, 17]. the gravity force in the earth frame according to [17] is: $F_{GI} = m[0 \quad 0 \quad g]_E^T$. Other forces like the Coriolis force from the earth, the wind, and Euler forces are considered as a disturbance, summarized as F_{DI} in the earth frame: $F_{DI} = [F_{dIx} \quad F_{dIy} \quad F_{dIz}]_E^T$. the inertia matrix of the aircraft is J so according to [3, 4, 17] is defined as the following form: $J = [J_{xx} \ 0 \ 0 \ ; 0 \ J_{yy} \ 0 \ ; 0 \ 0 \ J_{zz}]^T$; $J \epsilon R_{3\times3}$. m is the mass of hexacopter and l is the distance from CG to the center of the propeller. The attitude of the vehicle in the air change, by controlling the angular velocity of motors, then the thrust moment vector is defined as $M_T = [M_p \quad M_q \quad M_r]^T$, where M_p, M_q, M_r are the moments about the axes X_B, Y_B, Z_B in the body frame [3, 4, 17]. The aerodynamic moment is expressed by the following equation: $M_{AI} = K_{RI}.\Omega^2 = K_{RI}[\dot{\phi}^2 \quad \dot{\theta}^2 \quad \dot{\psi}^2]^T$, where K_{RI} is a diagonal matrix related to the rotational aerodynamic friction constant by the parameter K_r [15, 17]. Disturbance moment is the total of the disturbances affecting the torque around the aircraft axes expressed as $M_{DI} = [M_{dI\phi} \quad M_{dI\theta} \quad M_{dI\psi}]^T$. Propeller Gyroscopic effect $M_{gyro} = [-J_r\dot{\theta}\omega_r \quad J_r\dot{\phi}\omega_r \quad 0]^T$ [3], Where J_r is the rotational inertia of the propeller $[NmS^2]$ and the ω_r is the overall propeller speed $[rad/s]$, as $\omega_r = -\omega_1 + \omega_2 - \omega_3 + \omega_4 - \omega_5 + \omega_6$. Yaw counter moment is the differences in rotational acceleration of the propellers defined as $M_{counter} = [0 \quad 0 \quad J_r\dot{\omega_r}]^T$ [3]. When the transformation matrix for angular velocities $S \to I$ the hexacopter tends to the stable point, therefore the equations of the angular rate will be related to the earth frame, in addition to considering some assumptions as: $\frac{J_r}{J_x} = \frac{J_r}{J_y} = \frac{J_r}{J_z} \to 0$ is a small effect around zero, $a = \frac{k_t}{m} \to 0$ and $J_x = J_y$. Therefore, the equations that govern the translational and rotational motion with respect to the earth frame are shown in Eq. 1, The control input to the system is vector $U = [U_x \quad U_y \quad U_z \quad U_p \quad U_q \quad U_r]^T$.

$$\begin{pmatrix} \ddot{x} = U_x - \frac{k_t}{m}\dot{x} + \frac{F_{dIx}}{m} \\ \ddot{y} = U_y - \frac{k_t}{m}\dot{y} + \frac{F_{dIy}}{m} \\ \ddot{z} = U_z - \frac{k_t}{m}\dot{z} - g + \frac{F_{dIz}}{m} \end{pmatrix} \text{and} \begin{pmatrix} \ddot{\phi} = U_p + b_1\dot{\theta}\dot{\psi} + c_1\dot{\phi}^2 + \frac{M_{dI\phi}}{J_x} \\ \ddot{\theta} = U_q + b_2\dot{\phi}\dot{\psi} + c_2\dot{\theta}^2 + \frac{M_{dI\theta}}{J_y} \\ \ddot{\psi} = U_r + c_3\dot{\psi}^2 + \frac{M_{dI\psi}}{J_z} \end{pmatrix} \quad (1)$$

where

$$\begin{cases} U_p = \frac{M_p}{J_x} = \frac{\sqrt{3}\rho l c_T A R^2}{2J_x}(\omega_3^2 + \omega_6^2 - \omega_4^2 - \omega_5^2) = a_\phi(\omega_3^2 + \omega_6^2 - \omega_4^2 - \omega_5^2) \\ U_q = \frac{M_q}{J_y} = \frac{\rho l c_T A R^2}{2J_y}(\omega_3^2 + \omega_5^2 + 2\omega_1^2 - \omega_4^2 - \omega_6^2 - 2\omega_2^2) = a_\theta(\omega_3^2 + \omega_5^2 + 2\omega_1^2 - \omega_4^2 - \omega_6^2 - 2\omega_2^2) \\ U_r = \frac{M_r}{J_z} = \frac{\rho c_Q A R^3}{2J_z}(\omega_1^2 + \omega_4^2 + \omega_6^2 - \omega_2^2 - \omega_3^2 - \omega_5^2) = a_\psi(\omega_1^2 + \omega_4^2 + \omega_6^2 - \omega_2^2 - \omega_3^2 - \omega_5^2) \\ b_1 = \frac{(J_y - J_z)}{J_x}, b_2 = \frac{(J_z - J_x)}{J_y}, c_1 = -\frac{k_r}{J_x}, c_2 = -\frac{k_r}{J_y}, c_3 = -\frac{k_r}{J_z} \end{cases} \quad (2)$$

$$\begin{cases} U_x = (cos\phi cos\psi sin\theta + sin\phi sin\psi)\, u_T/m = a_x(\phi,\theta,\psi)\sum_{i=1}^{6}\omega_i^2 \\ U_y = (cos\phi sin\theta sin\psi - sin\phi cos\psi)\, u_T/m = a_y(\phi,\theta,\psi)\sum_{i=1}^{6}\omega_i^2 \\ U_z = (cos\phi cos\theta)\, u_T/m = a_z(\phi,\theta)\sum_{i=1}^{6}\omega_i^2 \\ u_T = \sum_{i=1}^{6}|T_i| = \rho C_T A R^2 \sum_{i=1}^{6}\omega_i^2 \end{cases} \quad (3)$$

4. State Space Model

The dynamic model presented in translational and rotational equation set can be rewritten in the state-space form: $\dot{X} = f(X) + g(X,U) + \delta$, where δ is the disturbances, and $X \epsilon \mathcal{R}^{12}$ is the vector of state variables given as follows: $X = [x \quad \dot{x} \quad y \quad \dot{y} \quad z \quad \dot{z} \quad \phi \quad \dot{\phi} \quad \theta \quad \dot{\theta} \quad \psi \quad \dot{\psi}]^T$, Then we can derive the final equations of the system, which governs the transitional and rotational of hexacopter, with respect to the earth frame in state space as follows:

$$\begin{pmatrix} \dot{x}_2 \\ \dot{x}_4 \\ \dot{x}_6 \end{pmatrix} = \begin{pmatrix} -a & 0 & 0 \\ 0 & -a & 0 \\ 0 & 0 & -a \end{pmatrix} \begin{pmatrix} x_2 \\ x_4 \\ x_6 \end{pmatrix} + \begin{pmatrix} U_x \\ U_y \\ U_z \end{pmatrix} + \begin{pmatrix} F_{dIx}/m \\ F_{dIy}/m \\ \frac{F_{dIz}}{m} - g \end{pmatrix} = \begin{pmatrix} U_x \\ U_y \\ U_z \end{pmatrix} + \begin{pmatrix} F_{dIx}/m \\ F_{dIy}/m \\ \frac{F_{dIz}}{m} - g \end{pmatrix} \quad (4)$$

$$\begin{pmatrix} \dot{x}_8 \\ \dot{x}_{10} \\ \dot{x}_{12} \end{pmatrix} = \begin{pmatrix} b_1 x_{10} x_{12} + c_1 x_8^2 \\ b_2 x_8 x_{12} + c_2 x_{10}^2 \\ b_3 x_8 x_{10} + c_3 x_{12}^2 \end{pmatrix} + \begin{pmatrix} 1 & 0 & 0 \\ 0 & 1 & 0 \\ 0 & 0 & 1 \end{pmatrix} \begin{pmatrix} U_p \\ U_q \\ U_r \end{pmatrix} + \begin{pmatrix} \frac{M_{dI\phi}}{J_x} \\ \frac{M_{dI\theta}}{J_y} \\ \frac{M_{dI\psi}}{J_z} \end{pmatrix} \quad (5)$$

The control input to the system is vector $U = [U_x \quad U_y \quad U_z \quad U_p \quad U_q \quad U_r]^T$, where the following equation Eq. 21 gives the relation between the angular speed of the propellers and the control inputs. The model of disturbances, which simulates the robotic arm, was presented as shown in Fig. 2. The final concluded equations represent nonlinearity, coupling and time-variance in the variables that are not considered in other papers like [3, 4], which use simplification techniques as well as linearization tools. Any change in the input variables leads to changes in most of the output variables. With respect to the control input vector U, it is clear that the rotational subsystem is fully-actuated, while the translational subsystem is underactuated as it is dependent on both the translational state variables x_1 to x_6 and the rotational ones x_7 to x_{12}.

$$\begin{bmatrix} U_x \\ U_y \\ U_z \\ U_p \\ U_q \\ U_r \end{bmatrix} = \begin{bmatrix} +a_x & +a_x & +a_x & +a_x & +a_x & +a_x \\ +a_y & +a_y & +a_y & +a_y & +a_y & +a_y \\ +a_z & +a_z & +a_z & +a_z & +a_z & +a_z \\ 0 & 0 & +a_\emptyset & -a_\emptyset & -a_\emptyset & +a_\emptyset \\ 2a_\theta & -2a_\theta & +a_\theta & -a_\theta & +a_\theta & -a_\theta \\ +a_\psi & -a_\psi & -a_\psi & +a_\psi & -a_\psi & +a_\psi \end{bmatrix} \cdot \begin{bmatrix} \omega_1^2 \\ \omega_2^2 \\ \omega_3^2 \\ \omega_4^2 \\ \omega_5^2 \\ \omega_6^2 \end{bmatrix} \quad (6)$$

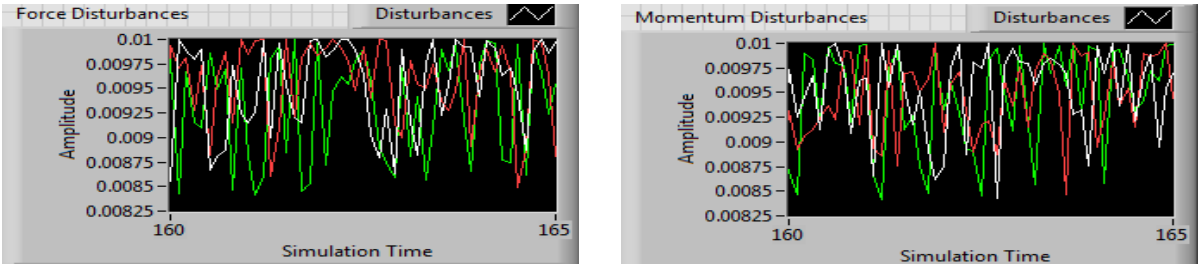

Figure 2. Force and momentum disturbances resulted from the robotic arm.

5. Proportion, Integral, And Derivative Controller Design

Four linear and classical PID controllers are presented, and their parameters were tuned using Ziegler Nichols algorithm [19]. The controllers speed here is considered suitable in a way that enables tracking the vibrations and changes in order to avoid the vibrations in the output of the aircraft as much as possible. The aim of these controllers is to control attitude and altitude of the vehicle at desired trajectory in space. The PID mathematical model is described as [19]:

$$u(t) = k_C[e(t) + \frac{1}{T_i}\int e(t).d(t) + T_d\frac{d}{dt}e(t)] \quad (7)$$

Parameter k_c is the proportional gain, T_i is the integral time, and T_d is the derivative time. These parameters are defined, in order to get the best performance by decreasing vibrations, steady-state errors, and response time. Fig. 3 shows a block diagram of PIDs controlling hexacopter. The parameters of each PID are defined as:

$$u_T(t) = 24.19\left[e(t) + \frac{1}{0.08299}\int e(t).d(t) + 0.01328\,\frac{d}{dt}e(t)\right] \quad (8)$$

$$u_p(t) = 0.001\left[e(t) + \frac{1}{6.1}\int e(t).d(t) + 0.1\,\frac{d}{dt}e(t)\right] \quad (9)$$

$$u_r(t) = -0.00103\left[e(t) + \frac{1}{6.3}\int e(t).d(t) + 0.04073\,\frac{d}{dt}e(t)\right] \quad (10)$$

$$u_y(t) = 0.006\left[e(t) + \frac{1}{20}\int e(t).d(t) + 0.4\,\frac{d}{dt}e(t)\right] \quad (11)$$

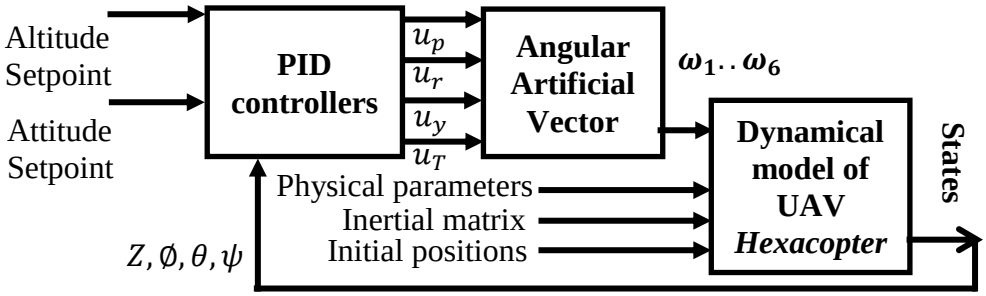

Figure 3. A block diagram of PIDs connected to Hexacopter model.

To control a hexacopter an application was conducted by LabVIEW using Runge-Kutta 2 method with a fixed step of 0.05 [sec]. The PID controllers were implemented to stabilize the altitude and attitude as shown from Fig. 4 to Fig. 8. The curves show the control signal and the fast response of the controllers with the existence of disturbances that emulate the existence of an arm in a non-laboratory environment. These controllers avoid the occurrence of vibrations in the output variables of the flying object as possible. The tuning process has been achieved after many experimental trials. Our scenario is the hovering flight at the altitude of multi-levels in the air according to table 1. The system's parameters, which has been used in the simulation model, are listed in table 2. Correlations were analyzed for all parameters of motion equations.

Table 1. Stability Response of PID Controllers.

PID Controller	Response Time [S]	Steady-State Error
Altitude	22.5	-0.0911 [m]
Pitch	8.15	0.01955 [deg]
Roll	5.72	0.0941 [deg]
Yaw	5.58	0.00173 [deg]

Table 2. Parameters used in the simulation.

m=4 [kg]	g=9.806 [m/s^2]	l=0.5 [m]
J_x,J_y=3.8e-4 [kg.m.s^2/rad]	R =0.15 [m]	k_t=4.8e-3 [kg.s/m]
J_z=7.1e-4 [kg.m.s^2/rad]	A =0.071 [m^2]	k_r=6.4e-5 [kg.m.s/rad]
C_T=0.01458	C_Q=1.037e-3	ρ=1.293 [kg/m^3]

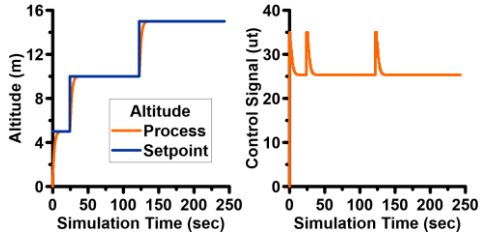

Figure 4. Stability response of altitude and control signal.

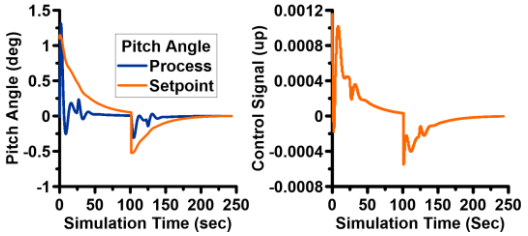

Figure 5. Stability response of pitch angle and control signal.

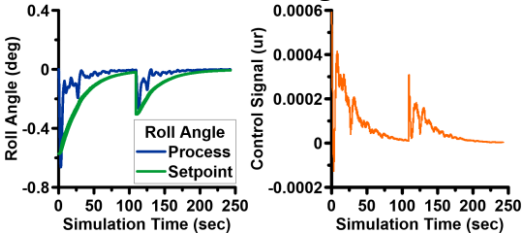

Figure 6. Stability response of roll angle and control signal.

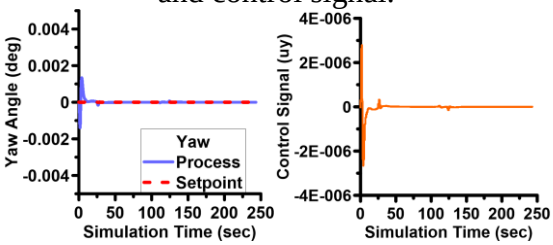

Figure 7. Stability response of yaw angle and control signal.

Figure 8. Stability response of X and Y coordinate systems.

6. Linear Quadratic Regulator

This kind of controller aims to minimize the following quadratic cost function [15, 16]:

$$J = \int_0^\infty [X^T(t).Q.X(t) + U^T(t).R.U(t)]dt$$

Using a feedback controller gain k such that $U(t) = -kX(t)$, where Q, R are weighting matrices. The task in LQR design is to choose appropriate weighting matrices. Where Q, R diagonal matrices, Q limit the amplitude of the state variables while R limit the amplitude of the inputs and these coefficients treat the optimization and energy terms in the model. The main goal is to make the vehicle reach its desired position as fast as possible. The state space representation of the dynamic model is $X = AX + BU + \delta_M$, Where: A is a state matrix, B is a input matrix, $X = [\emptyset \quad \theta \quad \psi \quad \dot{\emptyset} \quad \dot{\theta} \quad \dot{\psi}]^T$ is a state vector, $U = [M_p \quad M_q \quad M_r]^T$ is a control signal $\delta_M = [M_{dI\phi} \quad M_{dI\theta} \quad M_{dI\psi}]^T$ is disturbance vector of moments, and finally reference vector is $X_r = [\emptyset_r \quad \theta_r \quad \psi_r \quad \dot{\emptyset}_r \quad \dot{\theta}_r \quad \dot{\psi}_r]^T$. The LQR controller was implemented on a state vector to follow the reference vector. The model was linearized around the hover situation after decoupling the equations of motion in Eq. 1, and writing the stochastic state space model in addition to add disturbances to emulate the real motion in the sky. It is considered weak to make an approximation in describing the whole aircraft system in the state space, because the translational movement equations in the earth frame are dependent on the output of the rotational movement equations, therefore the system is divided into two state spaces. A linear–quadratic regulator (LQR) controller was designed only for the rotational movement. The random state space allows adding the disturbances to the model therefore it is considered closer to the real aircraft model, where its information is taken based on the covariance and mean calculations of previously studied disturbances' measurements. Fig. 9 illustrates the application of the LQR controller to the aircraft. The closed loop

simulation results using LabVIEW are shown on table (3). Fig. 10 shows the model's states after applying the LQR controller. Figures 11 and 12 show the results of applying the LQR controller and the control signals. The amplitude values of the control signals are very small in comparison to the PID controller, leading to reduction in the consumed power.

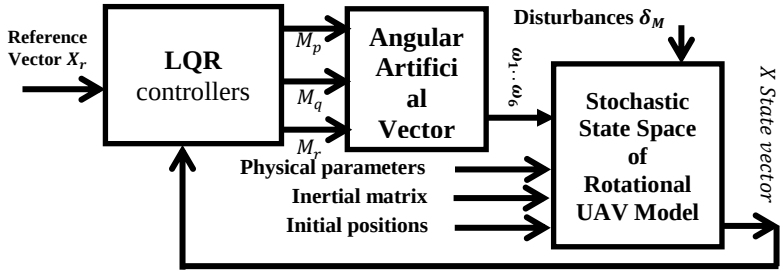

Figure 9. A block diagram of PIDs connected to Hexacopter model.

Table (3) Stability Response of LQR Controller.

Time Response Parametric Data	$\emptyset$	θ	ψ
Settling Time [s] is the time required for the response to reach 1% of its final value.	0.05	0.05	0.05
Rise Time [s] is the time required for the dynamic system response to rise from 10% of its final value to 90% of its final value.	0.05	0.05	0
Peak Time [s] is the time required for the dynamic system response to reach the peak value of its first overshoot.	0.05	0.05	0.05
Peak value returns the value at which the maximum absolute value of the time response occurs.	1.16842	1.16842	1.09014
Overshoot is the dynamic system response value that most exceeds unity, expressed as a percent.	1.75277E-5	1.75277E-5	1.87856E-5
Steady-State Gain is the final value of the signal after transient responses decay.	1.16842	1.16842	1.09014

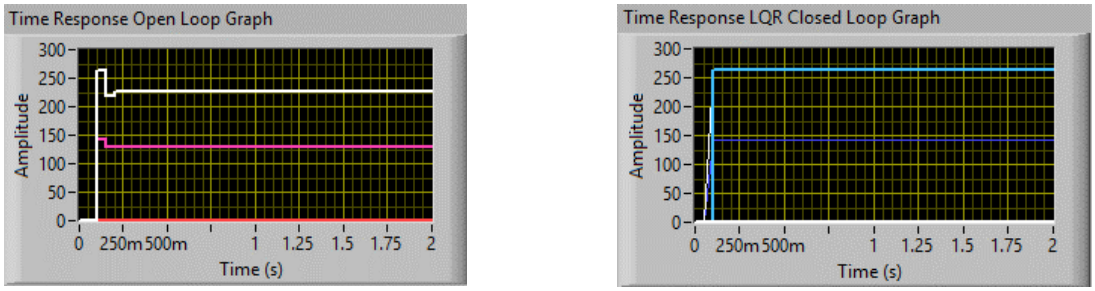

Figure (10). Time response of open and closed loop for stochastic state space model.

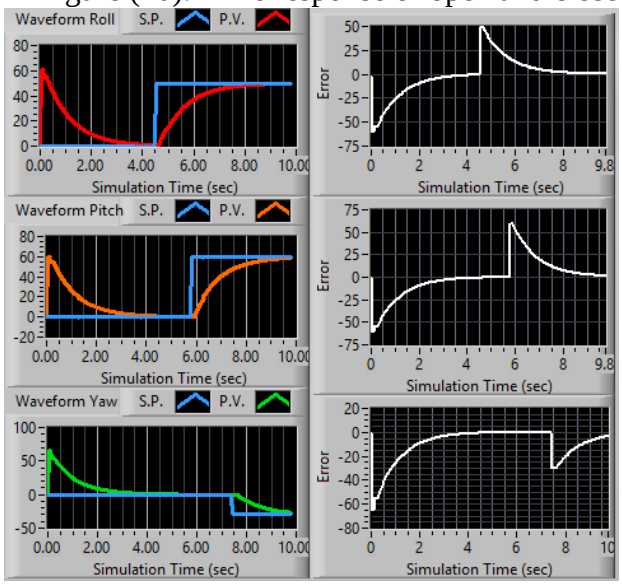

Figure (11). Stability response of roll, pitch and yaw angles and their error signals.

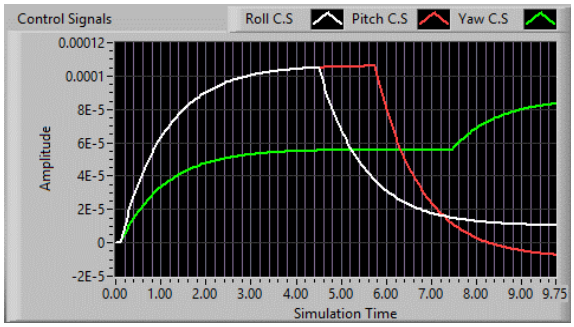

Figure (12). Control signals of LQR controller.

Conclusions

In this paper, the behavior of a hexacopter with the existence of disturbances inserted into the equations of motion was explored. These disturbances emulate the motion of a robotic arm attached to the body of the aircraft model. The derived dynamic model reflects the real motion of the hexacopter with respect to the earth, which is also characterized by nonlinearity, time variance, underactuation and coupling among the equations' variables. The state space method was used to write the equations in addition to decoupling and linearization techniques in order to design the controllers. Both PID and LQR controllers have been investigated to control the aircraft model. The results of comparison between them indicate that LQR controller is kind of an optimization technique and used to stabilize the attitude of the hexacopter. It consumes low energy with respect to the PID controller in addition to rejecting the perturbation and noise in the stochastic state space of the aircraft model.

References

[1] Bouadi, H., and M. Tadjine. "Nonlinear observer design and sliding mode control of four rotors helicopter." *Vorld Academy of Science, Engineering and Technology* 25 (2007): 225-229.

[2] Abas, Norafizah, Ari Legowo, and Rini Akmeliawati. "Parameter identification of an autonomous quadrotor." *Mechatronics (ICOM), 2011 4th International Conference On*. IEEE, 2011.

[3] Fogelberg, Johan. "Navigation and Autonomous Control of a Minicopter in Indoor Environments." *MSc Thesis, Department of Automatic Control, Lund University*, ISSN 0280-5316 (2013).

[4] Moussid, Mostafa, Adil Sayouti, and Hicham Medromi. "Dynamic Modeling and Control of a HexaRotor using Linear and Nonlinear Methods."*International Journal of Applied Information Systems* 9.5 (2015).

[5] Sanca, Armando S., P. J. Alsina, and F. Cerqueira Jés de Jesus. "Dynamic modeling with nonlinear inputs and backstepping control for a hexarotor Multi-aerial vehicle." *Robotics Symposium and Intelligent Robotic Meeting (LARS), 2010 Latin American*. IEEE, 2010.

[6] Di Lucia, Stefano, Gian Diego Tipaldi, and Wolfram Burgard. "Attitude stabilization control of an aerial manipulator using a quaternion-based backstepping approach." Mobile Robots (ECMR), 2015 European Conference on. IEEE, 2015.

[7] Ibrahim N. I., Oumran B., A Coupled and Underactuated Dynamic Model of Microcopter Using LabVIEW, IV Всероссийская научно-техническая конференция аспирантов, магистрантов и молодых ученых с международным участием (Young Scientists To Accelerate Scientific And Technological Progress In The Xxi Century), Ижевск 20 – 21 апреля 2016, PP. 981-990.

[8] Ibrahim N. I., Attitude and Altitude Stabilization of Microcopter using PID Controllers with Disturbances in LabVIEW, IV Всероссийская научно-техническая конференция аспирантов, магистрантов и молодых ученых с международным участием (Young Scientists To Accelerate Scientific And Technological Progress In The Xxi Century), Ижевск 20 – 21 апреля 2016, PP. 989-996.

[9] Bouabdallah, Samir, and Roland Siegwart. "Backstepping and sliding-mode techniques applied to an indoor micro quadrotor." Proceedings of the 2005 IEEE international conference on robotics and automation. IEEE, 2005.

[10] Grzonka S, Grisetti G, Burgard W. Towards a navigation system for autonomous indoor flying, In Robotics and Automation, 2009. ICRA'09. IEEE International Conference on 2009 May 12, pp. 2878-2883

[11] Bouabdallah, S., Murrieri, P. and Siegwart, R. (2005), "Towards autonomous indoor micro VTOL", Autonomous Robots, [Online], vol. 18, no. March, 2005, pp. 14/03/2007 available at: http://www.springerlink.com/content/llug3r141ll85726/fulltext.pdf.
[12] Bouabdallah, S., Murrieri, P. and Siegwart, R. (2004), "Design and control of an indoor micro quadrotor", 2004 IEEE International Conference on Robotics and Automation, April 2004, New Orleans, pp. 4393.
[13] Bouabdallah, S., Noth, A. and Siegwart, R. (2004), PID vs LQ control techniques applied to an indoor micro quadrotor, Swiss Federal Institute of Technology.
[14] Castillo, P., Lozano, R. and Dzul, A., (2005), Stabilization of a Mini Rotorcraft with Four Rotors, IEEE Control Systems Magazine.
[15] Hoffmann, G. M., Rajnarayan, D. G., Waslander, S. L., Dostal, D., Jang, J. S. and Tomlin, C. J. (2004), "The stanford testbed of autonomous rotorcraft for multi agent control", Digital Avionics Systems Conference, Vol. 2, 2004, pp. 12.E.4- 121-10.
[16] D. Julián, M. Colorado, *Towards Miniature MAV Autonomous Flight: A Modeling & Control Approach*, (Master thesis of Science in Robotics and Automation, Technical University of Madrid, April 2009).
[17] O. Magnussen, K. E. Skjonhaug, *Modeling, Design and Experimental Study for a Quadcopter System Construction* (Master Thesis in Faculty of technology and science, University of Agder-Kristiansand S, Norway, 2011).
[18] D. Sjoholm, M. Biel, *Automatic Control of a Quadrotor in the Smart Building* (KTH, School of Engineering Sciences (SCI), Master Thesis of Science in Engineering, KTH Royal Institute of Technology, 2014. Stockholm-Sweden, 2014).
[19] K. J. Astrom, R. M. Murray, *Feedback Systems* (Princeton University Press, ISBN-13: 978-0691135762, Vol.2, 11b, 2012).
[20] M. FABIÁN, R. BOSLAI, P. IŽOL, J. JANEKOVÁ, J. FABIANOVÁ, G. FEDORKO, P. BOŽEK. *Use of parametric 3D modelling* - tying parameter values to spreadsheets at designing molds for plastic injection. In Manufacturing technology. Vol. 15, No. 1 (2015), online, s. 24-31. ISSN 1213-2489.
[21] V. GOGA, P. BOŽEK. Application of INS to mechatronic systems control and regulation using virtual dynamic models. In *Proceedings of the 2013 International Conference on Process Control [elektronický zdroj] : Štrbské Pleso, Slovakia, June 18-21, 2013*. 1st. ed. Piscataway : IEEE, 2013, s.CD-ROM, p.185-189. ISBN 978-80-227-3951-1.
[22] P. BOŽEK. Control of a robotic arm on the principle of separate decision of an inertial navigation system. In *Applied Mechanics and Materials*. Vol. 611 (2014), s. 60-66. ISSN 1660-9336.
[23] P. BOŽEK, P. POKORNÝ, J. SVETLÍK, A. LOZHKIN, I. ARKHIPOV. The calculations of Jordan curves trajectory of the robot movement. In *International Journal of Advanced Robotic Systems*. Vol. 13, no. 5 (2016), online, [7]s. ISSN 1729-8806.
[24] M. Kelemen, I. Virgala, P. Frankovský, T. Kelemenová, L. Miková. Amplifying System for Actuator Displacement. International Journal of Applied Engineering Research, 11(15), (2016).8402-8407.
[25] M. Kelemen, I. Virgala, T. Kelemenová, Ľ. Miková, , P. Frankovský, T. Lipták, M. Lörinc, M. (2015). Distance Measurement via Using of Ultrasonic Sensor. Journal of Automation and Control, 3(3), 71-74.
[26] P. Frankovský, O. Ostertag, E. Ostertagová, F. Trebuňa, J. Kostka and M. Výrostek. (2017). Experimental analysis of stress fields of rotating structural elements by means of reflection photoelasticity. Applied Optics, 56(11), , 3064-3070.